Impurity effects on electronic transport in ferropnictide superconductors

Y. G. Pogorelov,[1] M. C. Santos,[2] and V. M. Loktev[3]
[1]*IFIMUP-IN, Departamento de Física, Universidade do Porto, Porto, Portugal*
[2]*Departamento de Física, Universidade de Coimbra, R. Larga, Coimbra 3004-535, Portugal*
[3]*Bogolyubov Institute for Theoretical Physics, NAS of Ukraine, 14b Metrologichna Street, 03143 Kiev, Ukraine*
(Received 19 August 2013; revised manuscript received 15 December 2013; published 31 December 2013)

Effects of impurities and disorder on transport properties by electronic quasiparticles in superconducting iron pnictides are theoretically considered. The most prominent new features compared to the case of pure material should appear at high enough impurity concentration when a specific narrow band of conducting quasiparticle states can develop within the superconducting gap, around the position of localized impurity level by a single impurity center. The predicted specific threshold effects in the frequency-dependent optical conductivity and temperature-dependent thermal conductivity and also in Seebeck and Peltier coefficients can have interesting potentialities for practical applications.

DOI: 10.1103/PhysRevB.88.224518 PACS number(s): 74.70.Xa, 74.62.Dh, 74.62.En

I. INTRODUCTION

A considerable interest in actual research of superconductivity (SC) with high critical temperature is focused on the family of doped ferropnictide compounds[1,2] and one of their notable distinctions from "old" BCS superconductors and more recent doped perovskite systems consists in the possibility for a peculiar, so-called extended s-wave symmetry of superconducting order parameter which changes its sign between electron and hole segments of the Fermi surface.[3] This additional property permits avoiding the fundamental limitation by the Anderson theorem[4] for nonmagnetic impurities to produce localized impurity levels within the superconducting band gap.[5,6] At finite, but low enough, impurity concentration, such levels are expected to give rise to some resonance effects like those well studied in semiconductors at low doping concentrations.[7] Analogous effects in superconductors were theoretically predicted and experimentally discovered for magnetic impurities, either in BCS systems[8–10] and in the two-band MgB_2 system.[11,12] In all those cases, the breakdown of the Anderson theorem is only due to the breakdown of the spin-singlet symmetry of an s-wave Cooper pair by a spin-polarized impurity, and the main physical interest of the considered case of SC iron pnictides from the point of view of disorder in general is the possibility for pair breaking even in nonmagnetic impurity[13–15] states and for related localized in-gap states.[16–19] This theoretical prediction was confirmed by the observations of various effects from localized impurity states, for instance, in the superfluid density (observed through the London penetration length),[20,21] transition critical temperature,[22,23] and electronic specific heat,[24] all mainly due to an emerging spike of electronic density of states against its zero value in the initial band gap.

But it is also known that indirect interactions between random impurity centers of a certain type (the so-called deep levels at high enough concentrations) in doped semiconductors can lead to formation of collective bandlike states.[25,26] This corresponds to the Anderson transition in a general disordered system,[27] and the emerging new band of quasiparticles in the spectrum can essentially change thermodynamics and transport in the doped material.[28] An intriguing possibility for similar banding of impurity levels within the SC gap[29,30] was recently discussed for the doped ferropnictides.[31] The present work is aimed at a more detailed analysis of the bandlike impurity states, focused on their observable effects that cannot be produced by localized impurity states. We use the specific form of Green's functions for superconducting quasiparticles derived in the previous work[31] in the general Kubo-Greenwood formalism[32] to obtain the temperature and frequency dependencies of optical and thermal conductivity and also of thermoelectric coefficients. These results are compared with the available experimental data and some suggestions are made on possible practical applications of such impurity effects.

II. GREEN'S FUNCTIONS FOR DISORDERED SC FERROPNICTIDE

We begin with a brief summary of the Green's function (GF) description of the electronic spectrum in LaOFeAs with impurities (not necessarily dopants) using the minimal coupling model[17,33] for the nonperturbed Hamiltonian. It considers only 2 types of local Fe orbitals, d_{xz} (or x) and d_{yz} (or y), on sites of a square lattice with lattice parameter a and 4 hopping parameters between nearest neighbors (NNs) and next-nearest neighbors (NNNs): (i) t_1 for xx or yy NNs along their orientations, and t_2 across them, and (ii) t_3 for xx or yy NNNs, and t_4 for xy NNNs. The resulting band Hamiltonian is diagonal in quasimomentum $\mathbf{k}$ and spin σ, but nondiagonal with respect to the orbital indices of the 2-spinors $\psi^\dagger(\mathbf{k},\sigma) = (x^\dagger_{\mathbf{k},\sigma}, y^\dagger_{\mathbf{k},\sigma})$:

$$H_t = \sum_{\mathbf{k},\sigma} \psi^\dagger(\mathbf{k},\sigma)\hat{h}(\mathbf{k})\psi(\mathbf{k},\sigma). \tag{1}$$

Here the energy matrix in orbital basis is expanded in Pauli matrices $\hat{\sigma}_i$: $\hat{h}(\mathbf{k}) = \varepsilon_{+,\mathbf{k}}\hat{\sigma}_0 + \varepsilon_{-,\mathbf{k}}\hat{\sigma}_3 + \varepsilon_{xy,\mathbf{k}}\hat{\sigma}_1$ with the energy factors $\varepsilon_{\pm,\mathbf{k}} = (\varepsilon_{x,\mathbf{k}} \pm \varepsilon_{x,\mathbf{k}})/2$, and

$$\varepsilon_{x,\mathbf{k}} = -2t_1 \cos ak_x - 2t_2 \cos ak_y - 4t_3 \cos ak_x \cos ak_y,$$
$$\varepsilon_{y,\mathbf{k}} = -2t_1 \cos ak_y - 2t_2 \cos ak_x - 4t_3 \cos ak_x \cos ak_y,$$
$$\varepsilon_{xy,\mathbf{k}} = -4t_4 \sin ak_x \sin ak_y.$$

It is readily diagonalized at passing from the orbital to subband basis: $\hat{h}_b(\mathbf{k}) = \hat{U}(\mathbf{k})\hat{h}(\mathbf{k})\hat{U}(\mathbf{k})^\dagger$, with the unitary matrix $\hat{U}(\mathbf{k}) = \exp(-i\hat{\sigma}_2\theta_\mathbf{k}/2)$ and $\theta_\mathbf{k} = \arctan(\varepsilon_{xy,\mathbf{k}}/\varepsilon_{-,\mathbf{k}})$. The resulting eigenenergies for electron and hole subbands are

$$\varepsilon_{h,e}(\mathbf{k}) = \varepsilon_{+,\mathbf{k}} \pm \sqrt{\varepsilon_{xy,\mathbf{k}}^2 + \varepsilon_{-,\mathbf{k}}^2}, \tag{2}$$

and respective electron and hole segments of the Fermi surface are defined by the equations $\varepsilon_{e,h}(\mathbf{k}) = \varepsilon_\mathrm{F}$. A reasonable fit to the LaOFeAs band structure by the more detailed LDA calculations[34] is attained with the parameter choice (in $|t_1|$ units) of $t_1 = -1$, $t_2 = 1.3$, $t_3 = t_4 = -0.85$.[35]

The SC state of such multiband electronic system is suitably described in terms of "multiband-Nambu" 4-spinors $\Psi_\mathbf{k}^\dagger = (\alpha_{\mathbf{k},\uparrow}^\dagger, \alpha_{-\mathbf{k},\downarrow}, \beta_{\mathbf{k},\uparrow}^\dagger, \beta_{-\mathbf{k},\downarrow})$ with the multiband spinor $(\alpha_{\mathbf{k},\sigma}^\dagger, \beta_{\mathbf{k},\sigma}^\dagger) = \psi^\dagger(\mathbf{k},\sigma)\hat{U}^\dagger(\mathbf{k})$, by a 4×4 extension of the Hamiltonian Eq. (1) in the form

$$H_s = \sum_{\mathbf{k},\sigma} \Psi_\mathbf{k}^\dagger \hat{h}_s(\mathbf{k}) \Psi_\mathbf{k}, \tag{3}$$

where the 4×4 matrix $\hat{h}_s(\mathbf{k}) = \hat{h}_b(\mathbf{k}) \otimes \hat{\tau}_3 + \Delta_\mathbf{k}\hat{\sigma}_0 \otimes \hat{\tau}_1$ includes the Pauli matrices $\hat{\tau}_i$ acting on the Nambu (particle-antiparticle) indices in Ψ-spinors. The simplified form for the extended s-wave gap function takes constant values $\Delta_\mathbf{k} = \Delta$ on the electron segments and $\Delta_\mathbf{k} = -\Delta$ on the hole segments.

The observable values result from the (Fourier transformed) GF 4×4 matrices $\hat{G}_{\mathbf{k},\mathbf{k}'} = \langle\langle \Psi_\mathbf{k} | \Psi_{\mathbf{k}'}^\dagger \rangle\rangle$, and for the nonperturbed system, Eq. (1), they are diagonal in quasimomentum: $\hat{G}_{\mathbf{k},\mathbf{k}'} = \delta_{\mathbf{k},\mathbf{k}'}\hat{g}_\mathbf{k}$ with

$$\hat{g}_\mathbf{k} = \frac{\varepsilon\hat{\tau}_0 + \varepsilon_e(\mathbf{k})\hat{\tau}_3 + \Delta\hat{\tau}_1}{2d_{e,\mathbf{k}}} \otimes \hat{\sigma}_e + \frac{\varepsilon\hat{\tau}_0 + \varepsilon_h(\mathbf{k})\hat{\tau}_3 - \Delta\hat{\tau}_1}{2d_{h,\mathbf{k}}} \otimes \hat{\sigma}_h, \tag{4}$$

$\hat{\sigma}_{e,h} = (\hat{\sigma}_0 \pm \hat{\sigma}_3)/2$, $d_{i,\mathbf{k}} = \varepsilon^2 - \varepsilon_i^2(\mathbf{k}) - \Delta^2$.

To simplify the treatment of impurity perturbations, the band structure is approximated to identical circular electron and hole Fermi segments of radius k_F around respective points $\mathbf{K}_{e,h}$ in the Brillouin zone and to similar linear dispersion of normal state quasiparticles near the Fermi level ε_F: $\varepsilon_e(\mathbf{k}) - \varepsilon_\mathrm{F} = \hbar v_\mathrm{F}(|\mathbf{k} - \mathbf{K}_e| - k_\mathrm{F})$ and $\varepsilon_h(\mathbf{k}) - \varepsilon_\mathrm{F} = -\hbar v_\mathrm{F}(|\mathbf{k} - \mathbf{K}_h| - k_\mathrm{F})$. Moreover, we shall describe the contributions of both segments to overall electronic properties by a single quasimomentum variable ξ that identifies electron $\xi_e = \varepsilon_e(\mathbf{k}) - \varepsilon_\mathrm{F}$ and hole $\xi_h = \varepsilon_h(\mathbf{k}) - \varepsilon_\mathrm{F}$ ones.

Next, the Hamiltonian of the disordered SC system is chosen as $H = H_s + H_{imp}$ including besides H_s, Eq. (3), the term due to nonmagnetic impurities[5] on random sites $\mathbf{p}$ in Fe square lattice with an on-site energy shift V (supposed positive without loss of generality). It is written in the multiband-Nambu spinor form as

$$H_{imp} = \frac{1}{N} \sum_{\mathbf{p},\mathbf{k},\mathbf{k}'} e^{i(\mathbf{k}'-\mathbf{k})\cdot\mathbf{p}} \Psi_\mathbf{k}^\dagger \hat{V}_{\mathbf{k},\mathbf{k}'} \Psi_{\mathbf{k}'}, \tag{5}$$

with the number N of unit cells in the crystal and the 4×4 scattering matrix $\hat{V}_{\mathbf{k},\mathbf{k}'} = V\hat{U}_\mathbf{k}^\dagger\hat{U}_{\mathbf{k}'} \otimes \hat{\tau}_3$. In the presence of this perturbation, the GFs can be expressed in specific forms depending on whether the considered quasiparticle energy falls into the range of bandlike or localized states. Namely, for bandlike states, the momentum diagonal GF,

$$\hat{G}_\mathbf{k} = \hat{G}_{\mathbf{k},\mathbf{k}} = \left(\hat{g}_\mathbf{k}^{-1} - \hat{\Sigma}_\mathbf{k}\right)^{-1}, \tag{6}$$

involves the self-energy matrix $\hat{\Sigma}_\mathbf{k}$ in the form of the so-called renormalized group expansion:[36]

$$\hat{\Sigma}_\mathbf{k} = c\hat{T}(1 + c\hat{B}_\mathbf{k} + \cdots). \tag{7}$$

This series in powers of impurity concentration c begins from the (k-independent) T matrix, $\hat{T} = \hat{V}(1 - \hat{G}\hat{V})^{-1}$. From the matrices $\hat{V} = \hat{V}_{\mathbf{k},\mathbf{k}} = V\hat{\tau}_3$ and $\hat{G} = N^{-1}\sum_\mathbf{k}\hat{g}_\mathbf{k} = \pi\varepsilon\rho_\mathrm{F}\hat{\tau}_0/\sqrt{\Delta^2 - \varepsilon^2}$ (with the Fermi density of states ρ_F and the henceforth omitted trivial factor $\hat{\sigma}_0$), the T-matrix explicit form is

$$\hat{T} = \frac{V}{1+v^2} \frac{v\varepsilon\sqrt{\Delta^2 - \varepsilon^2}\hat{\tau}_0 - (\Delta^2 - \varepsilon^2)\hat{\tau}_3}{\varepsilon^2 - \varepsilon_0^2}, \tag{8}$$

where $\varepsilon_0 = \Delta/\sqrt{1+v^2}$ defines the in-gap impurity levels[17] through the dimensionless impurity perturbation parameter $v = \pi\rho_\mathrm{F}V$. Inside the gap, the T matrix, Eq. (8), is a real function which can be approximated near the impurity levels $\pm\varepsilon_0$ as $\hat{T} \approx \gamma^2(\varepsilon\hat{\tau}_0 - \varepsilon_0\hat{\tau}_3)/(\varepsilon^2 - \varepsilon_0^2)$, with the effective coupling constant $\gamma^2 = V\varepsilon_0(v\varepsilon_0/\Delta)^2$. In contrary, outside the gap it is dominated by its imaginary part: $\mathrm{Im}\hat{T} = (\gamma^2/v\varepsilon_0)\varepsilon\sqrt{\varepsilon^2 - \Delta^2}/(\varepsilon^2 - \varepsilon_0^2)$.

The next terms besides unity in the brackets of Eq. (7) describe the effects of indirect interactions between impurities, with $\hat{B}_\mathbf{k}$ related to pairs and the omitted terms to groups of three and more impurities. The series convergence defines the energy ranges of bandlike states, delimited by the Mott mobility edges ε_c.[28] Within the bandlike energy ranges, the self-energy matrix can be safely approximated by the T matrix, $\hat{\Sigma}_\mathbf{k} \approx c\hat{T}$, and the dispersion laws for corresponding bands at given quasimomentum $\mathbf{k}$ are defined from the $\hat{G}_\mathbf{k}$ denominator:

$$D_\mathbf{k}(\varepsilon) = \det\hat{G}_\mathbf{k}^{-1}(\varepsilon) = \tilde{d}_{e,\mathbf{k}}(\varepsilon)\tilde{d}_{h,\mathbf{k}}(\varepsilon) = \left(\tilde{\varepsilon}^2 - \tilde{\xi}_e^2 - \Delta^2\right)\left(\tilde{\varepsilon}^2 - \tilde{\xi}_h^2 - \Delta^2\right), \tag{9}$$

with the renormalized energy and momenta forms

$$\tilde{\varepsilon} = \varepsilon\left(1 - \frac{cVv}{1+v^2}\frac{\sqrt{\Delta^2 - \varepsilon^2}}{\varepsilon^2 - \varepsilon_0^2}\right),$$

$$\tilde{\xi}_j = \xi_j - \frac{cV}{1+v^2}\frac{\Delta^2 - \varepsilon^2}{\varepsilon^2 - \varepsilon_0^2}.$$

The roots of the dispersion equation $\mathrm{Re}\ D_\mathbf{k}(\varepsilon) = 0$ define up to 8 subbands: 4 of them with energies near the roots of the nonperturbed denominators $d_{j,\mathbf{k}}$ in the e and h segments can be called "principal" or pr bands (they are similar to quasiparticles in the pure crystal); and the other 4, "impurity" or imp bands, with energies near $\pm\varepsilon_0$ in the same segments are only specific for disordered systems. The dispersion law for pr bands is presented in the ξ scale as

$$\varepsilon_{pr}(\xi) \approx \sqrt{\xi^2 + \Delta^2}, \tag{10}$$

and it only differs from the nonperturbed one by the finite linewidth $\Gamma(\varepsilon) \approx c\mathrm{Im}\hat{T}$, so that the validity range of Eq. (10) defined from the known Ioffe-Regel-Mott criterion,

$\xi d\varepsilon_b/d\xi \gtrsim \Gamma(\varepsilon_b(\xi))$,[28,37] is $\xi \gtrsim c/(\pi\rho_F)$. This defines the mobility edge in closeness to the gap edge,

$$\varepsilon_c - \Delta \sim c^2/c_0^{4/3}\Delta. \tag{11}$$

Here $c_0 = (\pi\rho_F\varepsilon_0)^{3/2}/(ak_F)\sqrt{2v/(1+v^2)}$ is the characteristic impurity concentration such that the impurity bands emerge just at $c > c_0$.[31] Their dispersion (in ξ) for the exemplar case of positive energies and e segment is approximated as

$$\varepsilon_{imp}(\xi) \approx \varepsilon_0 + c\gamma^2 \frac{\xi - \varepsilon_0}{\xi^2 + \xi_0^2}. \tag{12}$$

The formal upper limit energy by Eq. (12), $\varepsilon_+ = \varepsilon_0 + c\gamma^2/[2(\Delta + \varepsilon_0)]$, is attained at $\xi = \xi_+ = \varepsilon_0 + \Delta$ and the lower limit $\varepsilon_- = \varepsilon_0 - c\gamma^2/[2(\Delta - \varepsilon_0)]$ at $\xi_- = \varepsilon_0 - \Delta$. But in fact, this dispersion law is only valid until the related mobility edges $\varepsilon_{c,\pm}$ whose onset near the i-band edges is due to the higher terms in the group expansion, Eq. (7), and amounts to

$$\begin{aligned} \varepsilon_+ - \varepsilon_{c,+} &\sim (\varepsilon_{\max} - \varepsilon_0)\left(\frac{c_0}{c}\right)^4, \\ \varepsilon_{c,-} - \varepsilon_- &\sim (\varepsilon_0 - \varepsilon_{\min})\left(\frac{c_0}{c}\right)^4. \end{aligned} \tag{13}$$

These limitations restrict ξ to beyond some vicinities of the extremal points: $|\xi - \xi_\pm| \gtrsim \xi_\pm (c_0/c)^2$ (narrow enough at $c \gg c_0$). Another limitation is that ξ not be too far from these points: $|\xi - \xi_\pm| \lesssim \xi_\pm (c/c_0)^4$. A symmetric replica of Eq. (12) near $-\varepsilon_0$ at the e segment is the impurity subband with the dispersion law $-\varepsilon_i(\xi)$. Yet two more impurity subbands near the h segment are described in the unified ξ frame by the inverted dispersion laws $\pm\varepsilon_{imp}(-\xi)$. The overall composition of bandlike states in this frame is shown in Fig. 1. It is also important to notice that the above-described in-gap impurity band structure is only justified until it is narrow enough compared to the SC gap Δ itself. From Eq. (12), this requires that the impurity concentration stay well below the upper critical value

$$c_1 = \pi\rho_F\Delta\sqrt{1+v^2},$$

which can amount to about a few percent. In what follows, the condition $c \ll c_1$ is presumed.

At least, for $c < c_0$, all the in-gap states are localized and more adequately described by an alternative, the so-called nonrenormalized group expansion of $\hat{G}_\mathbf{k}$ (though this case is beyond the scope of the present study) while the principal bands are still defined by Eqs. (10) and (11).

In-gap impurity states, either localized and bandlike, can produce notable resonance effects on various thermodynamical properties of disordered superconductors, as transition critical temperature, London penetration length, electronic specific heat, etc.[31] But besides that, other effects, only specific for new quasiparticle bands, can be expected on kinetic properties of the disordered material, while the localized impurity states should have practically no effect on them. Such phenomena can be naturally described in terms of the above-indicated GF matrices as seen in what follows.

An important remark can yet be made on possible self-consistency corrections for the self-energy in Eq. (6) at the T-matrix level, as used in many known treatments of impurity effects (e.g., Ref. 15). Such corrections can be also explicitly included in our approach but they will not change essentially the obtained bandlike spectra when the group expansion, Eq. (7), is converging.[38] Otherwise, if there is no such convergence and a Mott-Anderson transition from bandlike to localized states takes place, the very concept of self-consistency is not justified and, if still applied, can lead to spurious results as unphysical broadening of narrow impurity peaks in the spectrum (these caveats were recognized either in a general context of disordered solids[39] and specifically for impurity effects in superconductors[40]).

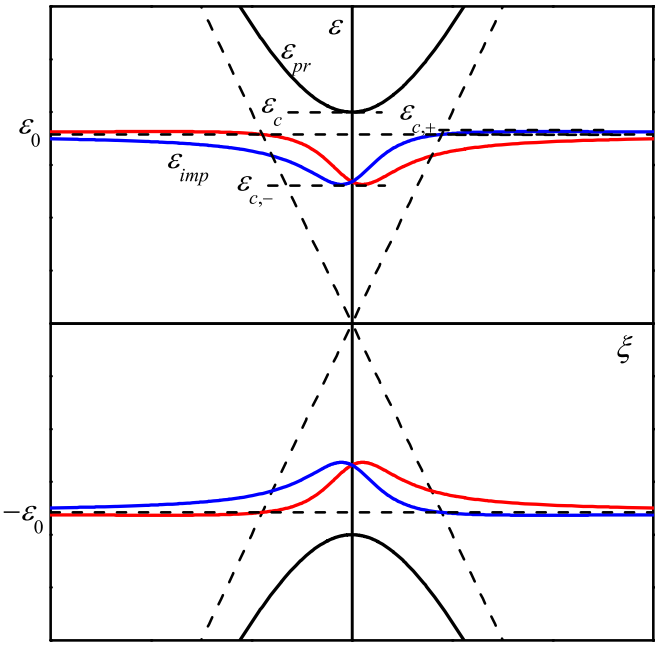

FIG. 1. (Color online) Dispersion laws in the modified quasiparticle spectrum of a SC ferropnictide with impurities. The impurity perturbation parameters were chosen as: $v = 0.5$, $c_0 = 1.3 \times 10^{-3}$, $c_1 = 1.7 \times 10^{-2}$, $c = 4 \times 10^{-3}$. For compactness, the plot superimposes the blue lines for the in-gap impurity subbands near the electron-like pockets of the Fermi surface and red lines for those near the hole-like pockets.

III. KUBO-GREENWOOD FORMALISM FOR MULTIBAND SUPERCONDUCTOR

The relevant kinetic coefficients for electronic processes in the considered disordered superconductor follow from the general Kubo-Greenwood formulation,[32] adapted here to the specific multiband structure of Green's function matrices. Thus, one of the basic transport characteristics, the (frequency and temperature dependent) electrical conductivity, is expressed in this approach as

$$\begin{aligned} \sigma(\omega,T) = \frac{e^2}{\pi}\int d\varepsilon \frac{f(\varepsilon) - f(\varepsilon')}{\omega}\int d\mathbf{k} v_x(\mathbf{k},\varepsilon)v_x(\mathbf{k},\varepsilon') \\ \times \mathrm{Tr}[\mathrm{Im}\hat{G}_\mathbf{k}(\varepsilon)\mathrm{Im}\hat{G}_\mathbf{k}(\varepsilon')], \end{aligned} \tag{14}$$

for $\varepsilon' = \varepsilon - \hbar\omega$ and the electric field applied along the x axis. Besides the common Fermi occupation function $f(\varepsilon) = (e^{\beta\varepsilon} + 1)^{-1}$ with the inverse temperature $\beta = 1/k_B T$, the

above formula involves the generalized velocity function:

$$\mathbf{v}(\mathbf{k},\varepsilon) = \left(\hbar\frac{\partial \mathrm{Re}D_{\mathbf{k}}(\varepsilon)}{\partial\varepsilon}\right)^{-1}\nabla_{\mathbf{k}}\mathrm{Re}D_{\mathbf{k}}(\varepsilon). \tag{15}$$

This function is defined in the whole ξ,ε plane in a way to coincide with the physical quasiparticle velocities for each particular band, Eqs. (9) and (12), along the corresponding dispersion laws: $\mathbf{v}(\mathbf{k},\varepsilon_j(\mathbf{k})) = \hbar^{-1}\nabla_{\mathbf{k}}\varepsilon_j(\mathbf{k}) = v_{j,\mathbf{k}}$, $j = p,i$. The conductivity resulting from Eq. (13) can be then used for calculation of optical reflectivity.

Other relevant quantities are the static (but temperature dependent) transport coefficients, as the heat conductivity:

$$\kappa(T) = \frac{\hbar}{\pi}\int d\varepsilon\frac{\partial f(\varepsilon)}{\partial\varepsilon}\varepsilon^2\int d\mathbf{k}[v_x(\mathbf{k},\varepsilon)]^2\,\mathrm{Tr}[\mathrm{Im}\hat{G}_{\mathbf{k}}(\varepsilon)]^2, \tag{16}$$

and the thermoelectric coefficients associated with the static electrical conductivity $\sigma(T) \equiv \sigma(0,T)$,[42] the Peltier coefficient:

$$\Pi(T) = \frac{\hbar e}{\pi\sigma(0,T)}\int d\varepsilon\frac{\partial f(\varepsilon)}{\partial\varepsilon}\varepsilon\int d\mathbf{k}\,[v_x(\mathbf{k},\varepsilon)]^2 \times \mathrm{Tr}[\mathrm{Im}\hat{G}_{\mathbf{k}}(\varepsilon)]^2, \tag{17}$$

and the Seebeck coefficient $S(T) = \Pi(T)/T$. All these transport characteristics, though being relatively more complicated from the theoretical point of view than the purely thermodynamical quantities as, e.g., specific heat or London penetration length,[31] permit an easier and more reliable experimental verification and so could be of higher interest for practical applications of the considered impurity effects in the multiband superconductors.

It is worth recalling that the above formulas are only contributed by the bandlike states; that is, the energy arguments ε,ε' in Eqs. (14)–(17) are delimited by the relevant mobility edges. This is the main distinction of our approach from existing treatments of impurity effects on transport in ferropnictide superconductors using the T-matrix approximation to a solution like Eq. (6) for the whole energy spectrum,[41] even for its ranges where the very concept of velocity, as Eq. (15), ceases to be valid.

Next, we consider the particular calculation algorithms for the expressions Eqs. (14), (16), and (17), beginning with the more involved case of dynamical conductivity, Eq. (14), and then reducing it to simpler static quantities, Eqs. (16) and (17).

IV. OPTICAL CONDUCTIVITY

The integral in Eq. (14) is dominated by the contributions from δ-like peaks of the $\mathrm{Im}\hat{G}_{\mathbf{k}}(\varepsilon)$ and $\mathrm{Im}\hat{G}_{\mathbf{k}}(\varepsilon')$ matrix elements. These peaks arise from the above dispersion laws, Eqs. (9) and (11), thus restricting the energy integration to the bandlike ranges: $|\varepsilon| > \varepsilon_c$ for the p bands and $\varepsilon_{c,-} < |\varepsilon| < \varepsilon_{c,+}$ for the i bands. Regarding the occupation numbers $f(\varepsilon)$ and $f(\varepsilon')$ at reasonably low temperatures $k_BT \ll \Delta,\varepsilon_0$, the most effective contributions correspond to positive ε values, either from *pr* or *imp* bands, and to negative ε' values from their negative counterparts, p' or i'. There are three general kinds of such contributions: (i) *pr*-*pr*′, due to transitions between the principal bands, similar to those in optical conductivity by the pure crystal (but with a slightly shifted frequency threshold: $\hbar\omega \geqslant 2\varepsilon_c$), (ii) *pr*-*imp*′ (or *imp*-*pr*′), due to combined transitions between the principal and impurity bands within the frequency range $\hbar\omega \geqslant \varepsilon_c + \varepsilon_{c,-}$, and (iii) *imp*-*imp*′, due to transitions between the impurity bands within a narrow frequency range of $2\varepsilon_{c,-} < \hbar\omega < 2\varepsilon_{c,+}$. The frequency-momentum relations for these processes and corresponding peaks are displayed in Fig. 2. The resulting optical conductivity reads $\sigma(\omega,T) = \sum_\nu \sigma_\nu(\omega,T)$ with ν = *pr*-*pr*′, *imp*-*imp*′, and *imp*-*pr*′.

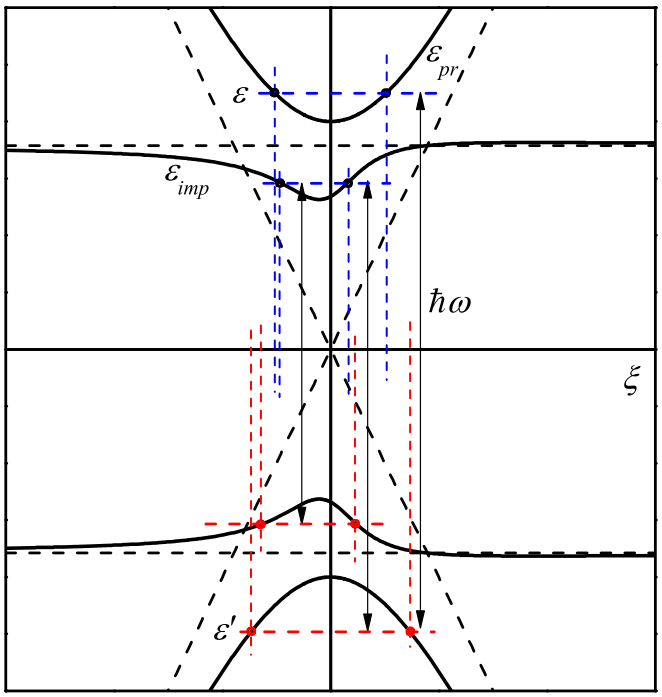

FIG. 2. (Color online) Configuration of the poles ξ_j of GFs contributing to different types of optical conductivity processes over one part (electronic pocket) of the quasiparticle spectrum by Fig. 1.

For practical calculation of each contribution, the relevant matrix $\mathrm{Im}\hat{G}_{\mathbf{k}}(\varepsilon)$ (within the bandlike energy ranges) can be presented as $\mathrm{Im}\hat{G}_{\mathbf{k}}(\varepsilon) = \hat{N}(\varepsilon,\xi)\mathrm{Im}[D_{\mathbf{k}}(\varepsilon)^{-1}]$ where the numerator matrix,

$$\hat{N}(\varepsilon,\xi) = \mathrm{Re}(\tilde{\varepsilon} + \tilde{\xi}\hat{\tau}_3 + \Delta\hat{\tau}_1), \tag{18}$$

is a smooth enough function while the peaks referred to above result from zeros of $\mathrm{Re}D_{\mathbf{k}}(\varepsilon)$. Now, the quasimomentum integration in Eq. (14) under the above-chosen symmetry of Fermi segments spells as $\int d\mathbf{k} = 2(hv_F)^{-1}\int d\varphi\int d\xi$ where the factor 2 accounts for identical contributions from e and h segments. The azimuthal integration contributes by the factor of π (from x projections of velocities) and the most important radial integration is readily done after expanding its integrand in particular pole terms:

$$v(\xi,\varepsilon)v(\xi,\varepsilon')\mathrm{Tr}[\mathrm{Im}\hat{G}(\xi,\varepsilon)\mathrm{Im}\hat{G}(\xi,\varepsilon')] = \sum_\alpha A_\alpha(\varepsilon,\varepsilon')\delta(\xi-\xi_\alpha), \tag{19}$$

where $v(\xi,\varepsilon) = |\mathbf{v}(\mathbf{k},\varepsilon)|$ and $\hat{G}(\xi,\varepsilon') \equiv \hat{G}_{\mathbf{k}}(\varepsilon')$ define the respective residues:

$$A_\alpha(\varepsilon,\varepsilon') = \pi v_\alpha v'_\alpha \frac{\tilde{\varepsilon}\tilde{\varepsilon}' + \tilde{\xi}\tilde{\xi}' + \Delta^2}{\prod_{\beta\neq\alpha}(\xi_\alpha - \xi_\beta)}. \tag{20}$$

Here $v_\alpha \equiv v(\varepsilon,\xi_\alpha)$, $v'_\alpha \equiv v(\varepsilon',\xi_\alpha)$, and the indices α,β run over all the poles of the two Green's functions. As follows from Eqs. (10) and (12) and seen in Fig. 2, there can be two such poles of $\hat{G}(\xi,\varepsilon)$ related to bandlike states with positive ε and respective quasimomentum values denoted as $\xi_{1,2}(\varepsilon)$. For energies within the *pr* band, $\varepsilon > \varepsilon_c$, they are symmetrical:

$$\xi_{1,2}(\varepsilon) \approx \pm\sqrt{\varepsilon^2 - \Delta^2}, \tag{21}$$

while within the *imp*-band at $\varepsilon_{c,-} < \varepsilon < \varepsilon_{c,+}$, their positions are asymmetrical:

$$\xi_{1,2}(\varepsilon) \approx \frac{c\gamma^2 \mp 2\varepsilon_0\sqrt{(\varepsilon_+ - \varepsilon)(\varepsilon - \varepsilon_-)}}{2(\varepsilon - \varepsilon_0)}. \tag{22}$$

Notice also that, within the *imp* band, there is a narrow vicinity of ε_0 of $\sim c_0^{1/3}(c_0/c)^3\varepsilon_0$ width where only the ξ_1 pole by Eq. (22) is meaningful and the other contradicts the Ioffe-Regel-Mott criterion (so that there are no bandlike states with that formal ξ_2 value in this energy range). Analogous poles of $\hat{G}(\xi,\varepsilon')$ at negative ε' are referred to as $\xi_{3,4}(\varepsilon')$ in what follows. Taking into account a nonzero $\mathrm{Im}D_{\mathbf{k}}(\varepsilon)$ [for the *imp* band, it is due to the nontrivial terms in the group expansion, Eq. (7)], each αth pole becomes a δ-like peak with an effective linewidth Γ_α but this value turns to be essential (and will be specified) only at calculation of static coefficients like Eqs. (16) and (17).

Since four peaks in Eq. (19) for optical conductivity are typically well separated, the ξ integration is trivially done considering them true δ functions; then the particular terms in $\sigma(\omega,T)$ follow as the energy integrals:

$$\sigma_\nu(\omega,T) = 2e^2\int_{\varepsilon_{\nu,-}}^{\varepsilon_{\nu,+}} d\varepsilon \frac{f(\varepsilon) - f(\varepsilon')}{\omega}\sum_{\alpha=1}^{4} A_\alpha(\varepsilon,\varepsilon'), \tag{23}$$

where ν takes the values *pr*-*pr*′, *imp*-*pr*′, or *imp*-*imp*′ and the limits $\varepsilon_{\nu,\pm}$ should assure that both ε and ε' are kept within the respective bandlike energy ranges.

Thus, in the *pr*-*pr*′ term, the symmetry of the poles $\xi_{1,2}(\varepsilon)$ and $\xi_{3,4}(\varepsilon')$ by Eq. (21) and the symmetry of *pr* and *pr*′ bands themselves define their equal contributions; then using simplicity of the generalized velocity function $v(\xi,\varepsilon) = \xi/\varepsilon$ and the nonrenormalized energy and momentum variables, $\tilde{\varepsilon} \to \varepsilon$, $\tilde{\xi} \to \xi$, the energy integration between the limits $\varepsilon_{pr\text{-}pr',-} = \varepsilon_c$ and $\varepsilon_{pr\text{-}pr',+} = \hbar\omega - \varepsilon_c$ provides its explicit analytic form as $\sigma_{pr\text{-}pr'}(\omega,T) = \sigma_{pr\text{-}pr'}(\omega,0) - \sigma_{pr\text{-}pr',T}(\omega)$. Here the zero-temperature limit value is

$$\sigma_{pr\text{-}pr'}(\omega,0) \approx \sigma_0\frac{2\omega_c}{\omega^2}\left\{\sqrt{4\omega^2 - \omega_c^2}\ln\left[2\frac{\omega(2\omega - \omega_c) + \sqrt{\omega(\omega - \omega_c)(4\omega^2 - \omega_c^2)}}{\omega_c^2} - 1\right]\right.$$
$$\left. + 2\omega\ln\left[2\frac{\omega - \sqrt{\omega(\omega - \omega_c)}}{\omega_c} - 1\right] - 2\sqrt{\omega(\omega - \omega_c)}\right\}, \tag{24}$$

with the characteristic scale $\sigma_0 = e^2/\Delta^2$ and simple asymptotics:

$$\sigma_{pr\text{-}pr'}(\omega,0) \approx (2/3)\sigma_0(\omega/\omega_c - 1)^{3/2}, \quad \omega - \omega_c \ll \omega_c,$$
$$\sigma_{pr\text{-}pr'}(\omega,0) \approx \sigma_0(32\omega_c/\omega)\ln(2\omega/\omega_c), \quad \omega \gg \omega_c,$$

with respect to the threshold frequency $\omega_c = 2\varepsilon_c/\hbar$, reaching the maximum value $\approx 1.19\sigma_0$ at $\omega \approx 2.12\omega_c$ as seen in Fig. 3. The (small) finite-temperature correction to the above value,

$$\sigma_{pr\text{-}pr',T}(\omega) \approx \sigma_0\frac{2\omega_c^2 e^{-\beta\Delta}}{\beta\hbar(\omega - \omega_c)\omega\sqrt{\Delta}}\left[\frac{\sqrt{\hbar\omega}}{\Delta}\left(1 - \frac{F(\sqrt{\beta\hbar(\omega - \omega_c)})}{\sqrt{\beta\hbar(\omega - \omega_c)}}\right) + \frac{\sqrt{2\Delta}}{\hbar\omega - \Delta}\left(\frac{\sqrt{\pi}}{2}\frac{\mathrm{erf}(\sqrt{\beta\hbar(\omega - \omega_c)})}{\sqrt{\beta\hbar(\omega - \omega_c)}} - e^{-\beta\hbar(\omega-\omega_c)}\right)\right], \tag{25}$$

involves the Dawson function $F(z) = \sqrt{\pi}e^{-z^2}\mathrm{erf}(iz)/(2i)$ and the error function $\mathrm{erf}(z)$.[43]

Calculation of the *imp*-*pr*′ term is more complicated because of the asymmetry of the *imp*-band poles $\xi_{1,2}(\varepsilon)$ by Eq. (22) and their nonequivalence to the symmetric poles $\xi_{3,4}(\varepsilon')$ of the *pr*′ band analogous to Eq. (21). More complicated expressions also define the generalized velocity function within the *imp*-band range,

$$\hbar v(\xi,\varepsilon) = \frac{c\gamma^2 - \xi(\varepsilon - \varepsilon_0)}{\varepsilon(\varepsilon - \varepsilon_0 - c\gamma^2/\varepsilon_0)}, \tag{26}$$

and the energy integration limits: $\varepsilon_{imp\text{-}pr',-} = \varepsilon_{c,-}$ and $\varepsilon_{imp\text{-}pr',+} = \min[\varepsilon_{c,+},\hbar\omega - \varepsilon_c]$. Then the function $\sigma_{imp\text{-}pr'}(\omega,T)$ follows from a numerical integration in Eq. (23) and, as seen in Fig. 3, it has a lower threshold frequency $\omega'_c = \varepsilon_c + \varepsilon_{c,-}$ than the *pr*-*pr*′ term. Above this threshold, it starts to grow linearly as $\sim(\omega/\omega'_c - 1)c^{5/2}c_0^{-5/3}\sigma_0$ and, for the impurity concentrations within the "safety range," $c \ll c_1 \sim c_0^{2/3}$, becomes completely dominated by the *pr*-*pr*′ function, Eq. (24), above its threshold ω_c.

Finally, the *imp*-*imp*′ term is obtained with a similar numerical routine on Eq. (23), using Eq. (22) either for the

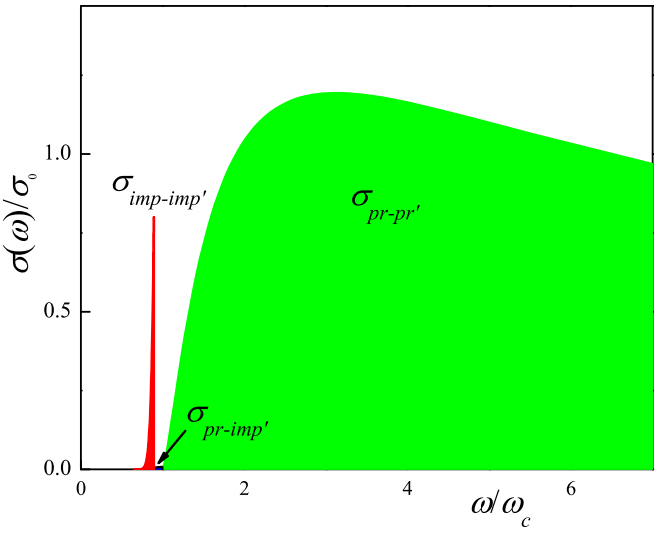

FIG. 3. (Color online) General picture of the optical conductivity showing three types of contributions.

poles $\xi_{1,2}(\varepsilon)$ by the *imp* band or for the $\xi_{3,4}(\varepsilon')$ by the *imp*′ band and Eq. (26) for respective generalized velocities, while the energy integration limits in this case are $\varepsilon_{imp\text{-}imp',-} = \varepsilon_{c,-}$ and $\varepsilon_{imp\text{-}imp',+} = \min[\varepsilon_{c,+}, \hbar\omega - \varepsilon_{c,-}]$. The resulting function $\sigma_{imp\text{-}imp'}(\omega, T)$ occupies the narrow frequency band from $\omega_{imp\text{-}imp',-} = 2\varepsilon_{c,-}/\hbar$ to $\omega_{imp\text{-}imp',+} = 2\varepsilon_{c,+}/\hbar$ (Fig. 3), and its asymptotics near these thresholds and in the zero-temperature limit are obtained analytically as

$$\sigma_{imp\text{-}imp'}(\omega,0) \approx \sigma_0 \frac{16c^{7/2}\gamma^7}{3\sqrt{2}\xi_-^7}\left(\frac{\omega-\omega_-}{\omega_-}\right)^{3/2}, \qquad (27)$$

at $0 < \omega - \omega_- \ll \omega_-$ and a similar formula for $0 < \omega_+ - \omega \ll \omega_+$ only differs from it by the change: $\xi_- \to \xi_+$ and $\omega_- \to \omega_+$.

Then the maximum contribution by the *imp*-*imp*′ term is estimated by extrapolation of the above asymptotics to the center of the impurity band: $|\omega - \omega_\pm| \sim |\omega_0 - \omega_\pm|$, resulting in $\sigma_{imp\text{-}imp',\max} \sim \sigma_0 c^5 c_0^{-10/3}(\xi_+/\xi_-)^{7/2}$. This estimate shows that the narrow *imp*-*imp*′ peak of optical conductivity around $\omega \approx 2\varepsilon_0/\hbar$ can, unlike the "combined" *imp*-*pr*′ term, become as intense as or even more so than the maximum of "principal" *pr*-*pr*′ intensity, Eq. (24), if the small factor $\sim(c/c_1)^5$ is overweighted by the next factor $(\xi_+/\xi_-)^{7/2}$. The latter is only possible if the impurity perturbation is *weak* enough: $v \ll 1$. Then the ratio ξ_+/ξ_- turns $\approx(2/v)^2 \gg 1$ and can really overweight the concentration factor if the impurity concentration c reaches $\sim c_1(v/2)^{7/5} \ll c_1$, which is quite realistic within the "safety" range $c \ll 1$. The overall picture of optical conductivity for an example of weakly coupled, $v = 0.25$, impurities at high enough concentration $c = 4c_0$ is shown in Fig. 3. The expressed effect of "giant" optical conductivity by the in-gap impurity excitations could be compared with the well-known Rashba enhancement of optical luminescence by impurity levels at closeness to the edge of the excitonic band[44] or with the huge impurity spin resonances in magnetic crystals,[36] but with a distinction that it appears here in a two-particle process instead of the above-mentioned single-particle ones.

It should be underlined again that the considered impurity features in optical conductivity cannot be interpreted in a simplistic view of optical transitions between localized impurity states (or between these and principal band states) since the lack of mobility for localized states would prevent their contribution to the currents. This is only recovered at high enough impurity concentrations, $c \gtrsim c_0$, when the impurity state banding takes place.

V. STATIC KINETIC COEFFICIENTS

Now we can pass to the relatively simpler calculation of the kinetic coefficients in the static limit of $\omega \to 0$. To begin with, consider the heat conductivity, Eq. (16), where the momentum integration at coincidence of the above-mentioned poles $\xi_{1.3}$ and $\xi_{2.4}$ is readily done using the general convolution formula,

$$\int L_{\Gamma_j}(\xi - \xi_j) L_{\Gamma'_k}(\xi - \xi'_k) d\xi = L_{\Gamma_j + \Gamma'_k}(\xi_j - \xi'_k), \qquad (28)$$

for two Lorentzian functions $L_\Gamma(\xi) = \Gamma/(\xi^2 + \Gamma^2)$, and in the limit of $\xi_i = \xi'_k$ and $\Gamma_j = \Gamma'_k$ obtaining simply $(2\Gamma_j)^{-1}$, a "combined lifetime." This immediately leads to a Drude-like formula for heat conductivity as a sum of principal and impurity terms, $\kappa(T) = \kappa_{pr}(T) + \kappa_{imp}(T)$, each of them given by

$$\kappa_{pr}(T) = \frac{\hbar(1+v^2)}{\pi c V v}\int_{\varepsilon_c}^{\infty} d\varepsilon \frac{\partial f(\varepsilon)}{\partial \varepsilon}\frac{\varepsilon\left(\varepsilon^2 - \varepsilon_0^2\right)}{\sqrt{\varepsilon^2 - \Delta^2}}$$
$$\approx \frac{\hbar\rho_F \Delta^2}{c}\sqrt{\frac{\pi\beta\Delta}{2}}\exp(-\beta\Delta) \qquad (29)$$

and

$$\kappa_{imp}(T) \approx \frac{\hbar}{\pi(\varepsilon_{c,+} - \varepsilon_{c,-})}\left(\frac{c}{c_0}\right)^4 \int_{\varepsilon_{c,-}}^{\varepsilon_{c,+}} d\varepsilon \frac{\partial f(\varepsilon)}{\partial \varepsilon}\varepsilon^2$$
$$\approx \frac{\hbar}{\pi}\left(\frac{c}{c_0}\right)^4 \beta\varepsilon_0^2 \exp(-\beta\varepsilon_0). \qquad (30)$$

Then the comparison of Eqs. (29) and (30) shows that the impurity contribution to the heat conductance κ_{imp} for impurity concentrations c above the critical value c_0 turns to dominate over the principal contribution κ_{pr} at all the temperatures (of course, below the critical transition temperature). Such strong impurity effect is combined from enhanced thermal occupation of impurity states and from their growing lifetime as $\sim c^3$ against the decreasing as $\sim 1/c$ lifetime in the principal band.

Similar strong impurity effects should also follow for the static electric conductivity $\sigma(0,T)$ (see Ref. 42) and for the thermoelectric Peltier and Seebeck coefficients, Eq. (17). All of them can be considered as fully due to the corresponding impurity contributions and the temperature dependencies of thermoelectric coefficients should be nonexponential: $\Pi(T) \approx \Pi(0) =$ constant, and $S(T) \approx \Pi(0)/T$, alike the nonperturbed case but at much higher level. Like the final note in the previous section, these predictions are only valid for impurity concentrations above the critical value, $c \gtrsim c_0$, while the system transport properties should stay almost nonaffected by impurities below this concentration, $c < c_0$. Figure 4 demonstrates these differences between temperature dependencies of static conductivities and of thermoelectric

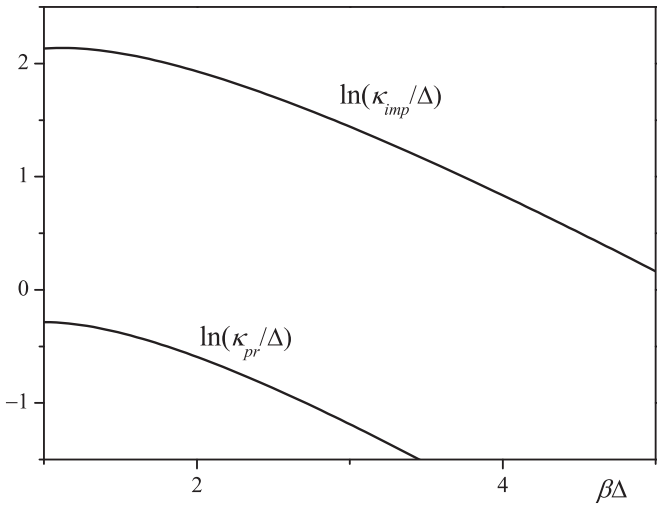

FIG. 4. Logarithmic plots for two contributions to the heat conductivity shows domination of the impurity term at all the temperatures where SC itself exists.

coefficients for low and high concentrations of impurities at the choice of perturbation parameter $v = 1$. Such drastic changes of transport behavior are of interest for experimental verification in properly prepared samples of SC ferropnictides with controlled concentration of specific impurities.

VI. CONCLUDING REMARKS

In conclusion, the essential modification of quasiparticle spectra in a SC ferropnictide with impurities of simplest (local and nonmagnetic) perturbation type is expected, consisting of formation of localized in-gap impurity states and their development into specific narrow bands of impurity quasiparticles at impurity concentration above a certain (quite low) critical value c_0 and leading to a number of effects in the system's observable properties. Besides the previously discussed thermodynamical effects, expected to appear at all impurity concentrations, which are due to either localized or bandlike impurity states, a special interest is seen in studying the impurity effects on electronic transport properties of such systems, only affected by the impurity bandlike states. It was shown above that the latter effects can be very strongly pronounced, either for high-frequency transport and for static transport processes. In the first case, the impurity effect is expected to most strongly be revealed in a narrow peak of optical conductance at its closeness to the edge of conductance band in nonperturbed crystal, resembling the known resonance enhancement of impurity absorption (or emission) processes near the edge of main quasiparticle band in normal systems; here it would be possible if the impurity perturbation were weak enough. The static transport coefficients at overcritical impurity concentrations are also expected to be strongly enhanced compared to those in a nonperturbed system, including the thermoelectric Peltier and Seebeck coefficients.

The above-presented simplest theoretical model can be extended to include either more realistic multiorbital structures of the initial ferropnictide system or more general types of impurity perturbation on it (e.g., as extended centers considered earlier in d-wave cuprate systems[45]). Of course, this can lead to some quantitative modifications of the results but their main qualitative features as a possibility for new narrow in-gap quasiparticle bands and related sharp resonant peaks in transport coefficients should be still present.

The experimental verifications of such predictions would be of evident interest, since they can open perspectives for important practical applications, e.g., in narrow-band microwave devices or advanced low-temperature sensors. However this would impose rather hard requirements on the quality and composition of the necessary samples; they should be extremely pure aside the extremely low (by common standards) and well-controlled contents of specially chosen and uniformly distributed impurity centers within the SC iron-arsenic planes of a ferropnictide compound. This situation can be compared to the requirements on doped semiconductor devices and hopefully should not be a real problem for modern laboratory technologies.

ACKNOWLEDGMENTS

Y.G.P. and M.C.S. acknowledge the support of this work through the Portuguese FCT Project No. PTDC/FIS/101126/2008. Also Y.G.P. recognizes the support from the Portuguese QREN Project No. Norte-070124-FEDER-000070. V.M.L. is grateful to the Special Program of Fundamental Research of the NAS of Ukraine.

[1] Y. Kamihara, H. Hiramatsu, M. Hirano, R. Kawamura, H. Yanagi, T. Kamiya, and H. Hosono, J. Am. Chem. Soc. **128**, 10012 (2006).
[2] Y. Kamihara, T. Watanabe, M. Hirano, and H. Hosono, J. Am. Chem. Soc. **130**, 3296 (2008).
[3] I. I. Mazin, D. J. Singh, M. D. Johannes, and M. H. Du, Phys. Rev. Lett. **101**, 057003 (2008).
[4] P. W. Anderson, J. Phys. Chem. Solids **11**, 26 (1959).
[5] D. Zhang, Phys. Rev. Lett. **103**, 186402 (2009).
[6] Y.-Y. Zhang, C. Fang, X. Zhou, K. Seo, W.-F. Tsai, B. A. Bernevig, and J. Hu, Phys. Rev. B **80**, 094528 (2009).
[7] B. I. Shklovskii and A. L. Efros, *Electronic Properties of Doped Semiconductors* (Springer-Verlag, Berlin, 1984).
[8] H. Shiba, Prog. Theor. Phys. **40**, 435 (1968).
[9] A. I. Rusinov, Sov. Phys. JETP **29**, 1101 (1969).
[10] K. Maki, Phys. Rev. **153**, 428 (1967).
[11] R. S. Gonnelli, D. Daghero, G. A. Ummarino, A. Calzolari, M. Tortello, V. A. Stepanov, N. D. Zhigadlo, K. Rogacki, J. Karpinski, F. Bernardini, and S. Massidda, Phys. Rev. Lett. **97**, 037001 (2006).
[12] C. P. Moca, E. Demler, B. Jankó, and G. Zaránd, Phys. Rev. B **77**, 174516 (2008).
[13] S. Onari and H. Kontani, Phys. Rev. Lett. **103**, 177001 (2009).
[14] H. Kontani and S. Onari, Phys. Rev. Lett. **104**, 157001 (2010).
[15] D. V. Efremov, M. M. Korshunov, O. V. Dolgov, A. A. Golubov, and P. J. Hirschfeld, Phys. Rev. B **84**, 180512 (2011).
[16] Y. Senga and H. Kontani, J. Phys. Soc. Jpn. **77**, 113710 (2008).

[17]W. F. Tsai, Y. Y. Zhang, C. Fang, and J. Hu, Phys. Rev. B **80**, 064513 (2009).
[18]T. Kariado and M. Ogata, J. Phys. Soc. Jpn. **79**, 083704 (2010).
[19]R. Beaird, I. Vekhter, and J.-X. Zhu, Phys. Rev. B **86**, 140507 (2012).
[20]R. T. Gordon, H. Kim, M. A. Tanatar, R. Prozorov, and V. G. Kogan, Phys. Rev. B **81**, 180501 (2010).
[21]S. Kitagawa, Y. Nakai, T. Iye, K. Ishida, Y. F. Guo, Y. G. Shi, K. Yamaura, and E. Takayama-Muromachi, Phys. Rev. B **83**, 180501(R) (2011).
[22]Y. F. Guo, Y. G. Shi, S. Yu, A. A. Belik, Y. Matsushita, M. Tanaka, Y. Katsuya, K. Kobayashi, I. Nowik, I. Felner, V. P. S. Awana, K. Yamaura, and E. Takayama-Muromachi, Phys. Rev. B **82**, 054506 (2010).
[23]Y. Li, J. Tong, Q. Tao, C. Feng, G. Cao, W. Chen, F. C. Zhang, and Z. A. Xu, New J. Phys. **12**, 083008 (2010).
[24]F. Hardy, P. Burger, T. Wolf, R. A. Fisher, P. Schweiss, P. Adelmann, R. Heid, R. Fromknecht, R. Eder, D. Ernst, H. v. Loehneysen, and C. Meingast, Europhys. Lett. **91**, 47008 (2010).
[25]M. A. Ivanov and Y. G. Pogorelov, JETP **61**, 1033 (1985).
[26]H. Yamamoto, Z.-Q. Fang, and D. C. Look, Appl. Phys. Lett. **57**, 1537 (1990).
[27]P. W. Anderson, Phys. Rev. **109**, 1492 (1958).
[28]N. F. Mott, Adv. Phys. **16**, 49 (1967).
[29]A. V. Balatsky, M. I. Salkola, and A. Rosengren, Phys. Rev. B **51**, 15547 (1995).
[30]V. M. Loktev and Y. G. Pogorelov, Low Temp. Phys. **27**, 767 (2001).
[31]Y. G. Pogorelov, M. C. Santos, and V. M. Loktev, Phys. Rev. B **84**, 144510 (2011).
[32]R. Kubo, J. Phys. Soc. Jpn. **12**, 570 (1957); D. A. Greenwood, Proc. Phys. Soc. **71**, 585 (1958).
[33]M. Daghofer, A. Moreo, J. A. Riera, E. Arrigoni, D. J. Scalapino, and E. Dagotto, Phys. Rev. Lett. **101**, 237004 (2008).
[34]G. Xu, W. Ming, Y. Yao, X. Dai, S. Zhang, and Z. Fang, Europhys. Lett. **82**, 67002 (2008).
[35]S. Raghu, X. L. Qi, C. X. Liu, D. J. Scalapino, and S. C. Zhang, Phys. Rev. B **77**, 220503 (2008).
[36]M. A. Ivanov, V. M. Loktev, and Y. G. Pogorelov, Phys. Rep. **153**, 209 (1987).
[37]A. F. Ioffe and A. R. Regel, Prog. Semicond. **4**, 237 (1960).
[38]Y. G. Pogorelov and V. M. Loktev, Phys. Rev. B **69**, 214508 (2004).
[39]R. J. Elliott, J. A. Krumhansl, and P. Leath, Rev. Mod. Phys. **46**, 465 (1974).
[40]V. M. Loktev and Y. G. Pogorelov, Phys. Lett. A **320**, 307 (2004).
[41]O. V. Dolgov, D. V. Efremov, M. M. Korshunov, A. Charnukha, A. V. Boris, and A. A. Golubov, J. Supercond. Nov. Magn. **26**, 2637 (2013).
[42]Note that this static limit of Eq. (13) only defines the conductivity by normal quasiparticles, seen, e.g., in normal resistivity by the magnetic flux flow in the mixed state, but otherwise short circuited by the infinite static conductivity due to supercurrents.
[43]M. Abramowitz and I. A. Stegun, *Handbook of Mathematical Functions* (National Bureau of Standards, Washington, DC, 1964).
[44]V. L. Broude, A. F. Prikhot'ko, and E. I. Rashba, Phys. Usp. **2**, 38 (1959).
[45]Y. G. Pogorelov and M. C. Santos, Phys. Rev. B **71**, 014516 (2005).